J|A|C|S COMMUNICATIONS

Published on Web 09/20/2010

Concave Cubic Gold Nanocrystals with High-Index Facets

Jian Zhang,[†,‡] Mark R. Langille,[†,‡] Michelle L. Personick,[‡] Ke Zhang,[‡] Shuyou Li,[§] and Chad A. Mirkin*[,‡,§]

Department of Chemistry, Department of Materials Science and Engineering, and International Institute for Nanotechnology, Northwestern University, 2145 Sheridan Road, Evanston, Illinois 60208

Received July 19, 2010; E-mail: chadnano@northwestern.edu

Abstract: A new class of gold nanostructures, concave nanocubes, enclosed by 24 high-index {720} facets, have been prepared in a monodisperse fashion by a modified seed-mediated synthetic method. The Cl^- counterion in the surfactant plays an essential role in controlling the concave morphology of the final product. The concave nanocubes exhibit higher chemical activities compared with low-index {111}-faceted octahedra.

As the field of nanotechnology evolves, it is becoming clear that particle shape is as important as size in determining the chemical and physical properties of a particular nanostructure. This is especially true for noble metal nanoparticles, where the plasmonic and catalytic properties can be finely tuned through control over their morphology.[1−7] Indeed, a variety of metallic nanostructures with well-defined shapes have been synthesized via photochemical,[1,8−11] thermal,[12−14] electrochemical,[15] and template-directed methods.[2,16] These synthetic strategies provide a means to chemically control the morphology of particles and, consequently, their catalytic, optical, electrical, and magnetic properties.[4−6] In the case of catalysis, not only the shape of the particle but also the exposed crystalline faces are important, which can have a marked influence on both activity and selectivity.[17,18] Interestingly, most synthetic methods to date yield nanostructures with convex shapes enclosed by low-index {111}, {100}, and/or {110} facets, and there are very few methods[19−22] that allow one to realize nanostructures with high-index faces. Herein, we describe how seed-mediated methods, originally developed by Murphy et al.[23,24] and El-Sayed et al.,[25] can be modified with the appropriate surfactant to yield a novel class of high-index {720}-faceted Au concave nanocubes.

In a typical synthesis, Au seeds were prepared by reduction of $HAuCl_4$ by $NaBH_4$ in the presence of cetyltrimethylammonium chloride (CTAC) instead of the conventional cetyltrimethylammonium bromide (CTAB). A growth solution was prepared by consecutively adding 0.5 mL of 10 mM $HAuCl_4$, 0.1 mL of 10 mM $AgNO_3$, 0.2 mL of 1.0 M HCl, and then 0.1 mL of 100 mM ascorbic acid (AA) to a 10 mL aqueous solution of 0.1 M CTAC. Concave Au nanocube synthesis was initiated by adding the seed particles to the growth solution (Supporting Information). The reaction was gently shaken immediately after the addition of the seeds and left undisturbed overnight. In general, the amount of seed particles added affects the size of the resulting concave nanocubes, with fewer seeds (i.e., fewer nucleation sites) leading to larger structures (*vide infra*).

The reaction products were extensively characterized by SEM and TEM (Figure 1). When the products lie flat on a substrate, the

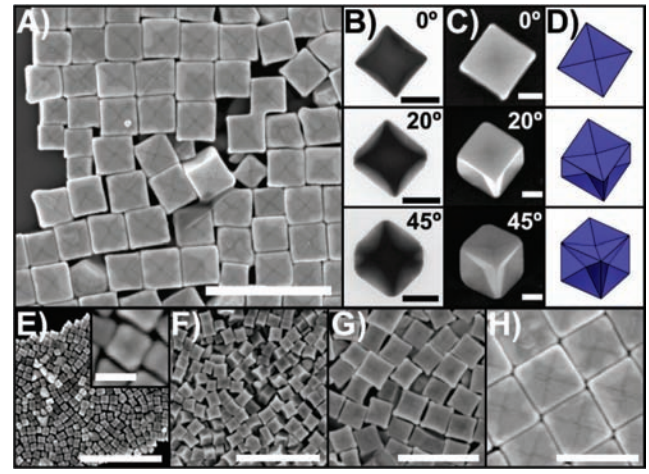

Figure 1. (A) Typical SEM image of Au concave cubes. Scale bar: 500 nm. (B) TEM, (C) SEM, and (D) model images of a concave cube tilted 0°, 20°, and 45° to illustrate the concave faces. Scale bars: 200 nm. SEM images of concave cubes with edge lengths of (E) 38 ± 7, (F) 69 ± 8, (G) 115 ± 19, and (H) 269 ± 18 nm. Particle size was determined from >100 particles in each sample. Scale bars: 500 nm. The inset of (E) shows a higher-magnification view, scale bar: 40 nm.

Au nanoparticles appear to have a cubic morphology. However, the SEM images (Figure 1A) show that the faces of the cubes each have contrast lines in the shape of an "X", and in the TEM images (Figure 1B) the cubes exhibit darker contrast in the middle region as compared with the edges. Incident beam angle-dependent TEM and SEM images show that each face of the cube is concave rather than flat (Figure 1B and 1C), and every particle inspected (>1000) has these concave faces.

Remarkably, the size of the concave nanocubes, as determined by edge length, can be adjusted from tens to hundreds of nanometers by varying the volume of seed particles added to the growth solution. Therefore, concave cubes with edge lengths of 38 ± 7, 69 ± 7, 115 ± 19, or 269 ± 18 nm can be synthesized (Figure 1E−H). SEM images of these products show that the concave faces of the cubes are maintained regardless of particle size, although the facets are better defined or more easily assignable for larger particles. A high yield (>95%) of the concave cubes was observed for all nanocube sizes studied. The UV−vis spectroscopy of the smaller concave cubes (Figure S1) is consistent with the shape determined by TEM; the plasmon resonance is red-shifted by 80 nm compared to cubes with flat surfaces and of similar dimensions.[26] Indeed, theory suggests that the plasmon resonance for the concave cubes, which have sharper tips than cubes with flat faces, is expected to be red-shifted.[1]

To fully characterize the novel structure of the concave nanocubes, it is important to index the surface facets. Due to the difficulty of directly imaging the concave faces, it was necessary to cut the

[†] These authors contributed equally.
[‡] Department of Chemistry and International Institute for Nanotechnology.
[§] Department of Materials Science and Engineering.

10.1021/ja106394k

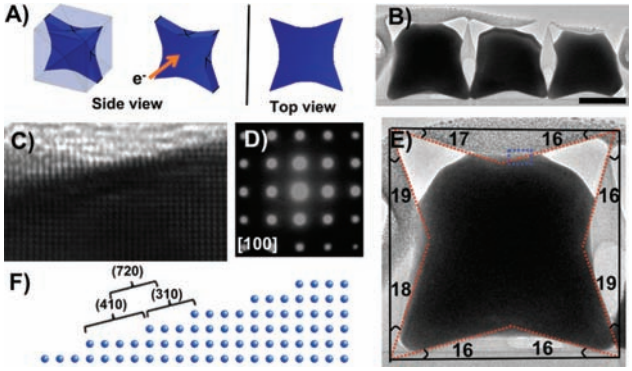

Figure 2. (A) Model and (B) TEM image of cross-sectioned concave cubes (scale bar: 200 nm). (C) HRTEM image of the edge of the high-index facet. (D) Electron diffraction pattern of the sectioned concave cube in (C). (E) Zoomed-in image of a single cut concave cube aligned edge-on. (F) Atomic model of the {720} surface, projected from the [001] direction, corresponding to the region indicated with a box in (E).

crystal so that the concave facets can be imaged edge-on. To accomplish this difficult task, we utilized a focused ion beam (FIB) to cut the particle and expose a cross section of the concave cube along the [001] direction. The remaining section was then tilted to the [100] direction, as confirmed by electron diffraction (Figure 2D). Note that parts of the thin tips were lost during transfer and mounting of the sample for TEM analysis. The projected image fits well with the model (Figure 2A). The angles between the facets of the concave cube and the (100) facets of an ideal cube were determined to be 17°, 16°, 16°, 19°, 16°, 16°, 18°, and 19°, respectively (Figure 2E). Similar results were also obtained from the two other concave cubes. The average measured angle is 17 ± 1°, indicating that the facets of the concave cubes are indeed high-index {720} facets, which have a calculated angle of 16.0°. Note that some facets appear to have a slightly larger angle such as 18°−19°, which can be attributed to a different high-index facet: {310}. Overall, we believe the facets of the concave cubes are mostly {720} planes, mixed with some {310} planes. A similar observation has also been made for the electrochemically prepared Pt tetrahexahedral nanoparticles, where, in addition to the most prevalent {730} planes, a few other planes such as {520}, {210}, and {310} planes were also identified.[19] The atomic arrangement of the {720} planes was further confirmed using high-resolution TEM (HR-TEM) (Figure 2C). The {720} facet is multiply stepped and composed of {410} and {310} subfacets (Figure 2F).

Nanostructures with concave faces are not common.[21,27,28] The concave nanocubes reported here can be viewed as cubes with the centers of the six square faces "pushed in" to generate square pyramid-shaped depressions. This yields a nanostructure enclosed by 24 facets. It was recently reported that when CTAB rather than CTAC was used, tetrahexahedral (THH) Au nanoparticles were obtained even though the rest of the conditions were identical.[22] Interestingly, the THH morphology can also be viewed as a cube with the centers of the six square faces "pulled out" to generate convex square pyramids (Figure 3). We have discovered that a simple change of the halide counterion in the surfactant induces a dramatic change in the product morphology and yields a concave rather than convex cubic structure.

Although the formation mechanism is, as of now, unclear, we believe that it is the combination of Ag^+ and Cl^- that gives rise to the concave cube morphology. Ag^+ has been used in other seed-mediated syntheses to stabilize high-index facets through an underpotential deposition (UPD) mechanism.[29] Interestingly, it was found in correlated scanning tunneling microscopy/cyclic voltammetry experiments that the presence of Cl^- significantly affects the UPD behavior of Ag^+ onto Au, with Ag^+ being deposited specifically onto atomic steps below a Cl^- adlayer, making the Ag^+ more difficult to remove.[30,31] While both CTAB and CTAC have been used to synthesize nanostructures with high-index facets,[21,22,29] CTAC has been attributed to the generation of nanoparticles with stellated features.[21,32] Efforts aimed at understanding the role of the halide in the particle growth pathway are underway.

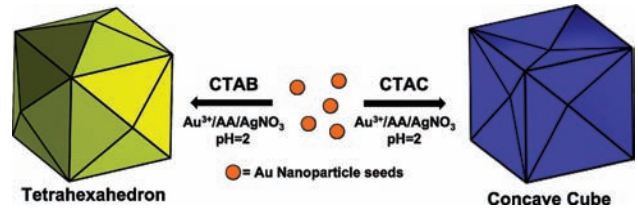

Figure 3. Schematic illustration showing the effect of the counterion on product morphology in the seed-mediated synthesis: CTAC leads to the formation of concave cubes, and CTAB leads to the formation of tetrahexahedra (convex cubes).

Concave Au cubes should have higher chemical activities than nanoparticle morphologies bound with low-index facets, due to the steps of the high-index {720} facets. Cyclic voltammetry (CV) is a method commonly used to study the surface structure of bulk Au,[33,34] and recently, this method has also been used to characterize the surface facets of Au nanostructures.[21,22] The CV traces of the concave cubes with different sizes exhibit oxidation peaks around 1.2 ± 0.5 V (Figure S2). This value is comparable to the result obtained for the THH Au nanoparticles enclosed by {730} facets, which was measured to be 1.18 V.[22] For comparison, the oxidation peak of octahedral Au nanoparticles (edge length 80 nm) was determined to be 1.43 V (Figure S2). The oxidation peak, which is at a lower potential for the concave cubes than the octahedra, indicates that the surface atoms of the concave cubes are easier to oxidize. This is likely a consequence of the {720} facets having a more open atomic arrangement as compared to the more tightly packed {111} facets of the octahedra. This result clearly demonstrates higher activity for the higher-indexed concave cubes.

In conclusion, we have discovered a new class of Au nanoparticles, which have been characterized as concave nanocubes. These structures are related to their convex counterparts, tetrahexahedra, and are made simply by changing the counterion of the surfactant used in the seed-mediated synthesis. Extensive electron microscopy studies show that the concave nanocubes are single crystals enclosed by 24 high-index {720} facets, and electrochemical measurements show that they are more chemically active (more susceptible to oxidation) than octahedral nanoparticles enclosed by low-index {111} facets. Therefore, these structures may become useful candidates for fundamental structure versus function catalytic studies.

Acknowledgment. This work was supported by the MRSEC program of the National Science Foundation at the Material Research Center of Northwestern University. The microscopy work was performed in the EPIC facility of NUANCE Center at Northwestern University. NUANCE Center is supported by NSF-NSEC, NSF-MRSEC, the Keck Foundation, the State of Illinois, and Northwestern University. We thank Ben Meyers for assistance with the FIB experiments. C.A.M. is also grateful for an NSSEF Fellowship from the DoD and support from the AFOSR.

Supporting Information Available: Experimental details, UV−vis extinction spectra, and cyclic voltammograms of different sized concave

nanocubes and octahedra. This material is available free of charge via the Internet at http://pubs.acs.org.

References

(1) Jin, R. C.; Cao, Y. W.; Mirkin, C. A.; Kelly, K. L.; Schatz, G. C.; Zheng, J. G. *Science* **2001**, *294*, 1901.
(2) Hurst, S. J.; Payne, E. K.; Qin, L. D.; Mirkin, C. A. *Angew. Chem., Int. Ed.* **2006**, *45*, 2672.
(3) Millstone, J. E.; Park, S. H.; Shuford, K. L.; Qin, L. D.; Schatz, G. C.; Mirkin, C. A. *J. Am. Chem. Soc.* **2005**, *127*, 5312.
(4) Millstone, J. E.; Hurst, S. J.; Métraux, G. S.; Cutler, J. I.; Mirkin, C. A. *Small* **2009**, *5*, 646.
(5) Xia, Y. N.; Xiong, Y. J.; Lim, B. K.; Skrabalak, S. E. *Angew. Chem., Int. Ed.* **2009**, *48*, 60.
(6) Tao, A. R.; Habas, S.; Yang, P. D. *Small* **2008**, *4*, 310.
(7) Somorjai, G. A.; Frei, H.; Park, J. Y. *J. Am. Chem. Soc.* **2009**, *131*, 16589.
(8) Maillard, M.; Huang, P. R.; Brus, L. *Nano Lett.* **2003**, *3*, 1611.
(9) Jin, R. C.; Cao, Y. C.; Hao, E. C.; Métraux, G. S.; Schatz, G. C.; Mirkin, C. A. *Nature* **2003**, *425*, 487.
(10) Xue, C.; Mirkin, C. A. *Angew. Chem., Int. Ed.* **2007**, *46*, 2036.
(11) Zhang, J.; Li, S. Z.; Wu, J. S.; Schatz, G. C.; Mirkin, C. A. *Angew. Chem., Int. Ed.* **2009**, *48*, 7787.
(12) Sun, Y. G.; Xia, Y. N. *Science* **2002**, *298*, 2176.
(13) Kim, F.; Connor, S.; Song, H. J.; Kuykendall, T.; Yang, P. D. *Angew. Chem., Int. Ed.* **2004**, *43*, 3673.
(14) Wang, C.; Daimon, H.; Onodera, T.; Koda, T.; Sun, S. H. *Angew. Chem., Int. Ed.* **2008**, *47*, 3588.
(15) Yu, Y. Y.; Chang, S. S.; Lee, C. L.; Wang, C. R. C. *J. Phys. Chem. B* **1997**, *101*, 6661.
(16) Martin, C. R. *Science* **1994**, *266*, 1961.
(17) Somorjai, G. A.; Blakely, D. W. *Nature* **1975**, *258*, 580.
(18) Sun, S. G.; Chen, A. C.; Huang, T. S.; Li, J. B.; Tian, Z. W. *J. Electroanal. Chem.* **1992**, *340*, 213.
(19) Tian, N.; Zhou, Z. Y.; Sun, S. G.; Ding, Y.; Wang, Z. L. *Science* **2007**, *316*, 732.
(20) Tian, N.; Zhou, Z. Y.; Sun, S. G. *J. Phys. Chem. C* **2008**, *112*, 19801.
(21) Ma, Y. Y.; Kuang, Q.; Jiang, Z. Y.; Xie, Z. X.; Huang, R. B.; Zheng, L. S. *Angew. Chem., Int. Ed.* **2008**, *47*, 8901.
(22) Ming, T.; Feng, W.; Tang, Q.; Wang, F.; Sun, L. D.; Wang, J. F.; Yan, C. H. *J. Am. Chem. Soc.* **2009**, *131*, 16350.
(23) Jana, N. R.; Gearheart, L.; Murphy, C. J. *J. Phys. Chem. B* **2001**, *105*, 4065.
(24) Sau, T. K.; Murphy, C. J. *J. Am. Chem. Soc.* **2004**, *126*, 8648.
(25) Nikoobakht, B.; El-Sayed, M. A. *Chem. Mater.* **2003**, *15*, 1957.
(26) Dovgolevsky, E.; Haick, H. *Small* **2008**, *4*, 2059.
(27) Zhou, Z. Y.; Tian, N.; Huang, Z. Z.; Chen, D. J.; Sun, S. G. *Faraday Discuss.* **2008**, *140*, 81.
(28) Huang, X. Q.; Tang, S. H.; Zhang, H. H.; Zhou, Z. Y.; Zheng, N. F. *J. Am. Chem. Soc.* **2009**, *131*, 13916.
(29) Liu, M. Z.; Guyot-Sionnest, P. *J. Phys. Chem. B* **2005**, *109*, 22192.
(30) Lee, J. H.; Oh, I. W.; Hwang, S. P.; Kwak, J. Y. *Langmuir* **2002**, *18*, 8025.
(31) Michalitsch, R.; Palmer, B. J.; Laibinis, P. E. *Langmuir* **2000**, *16*, 6533.
(32) Wu, H. L.; Chen, C. H.; Huang, M. H. *Chem. Mater.* **2009**, *21*, 110.
(33) Hamelin, A. *J. Electroanal. Chem.* **1996**, *407*, 1.
(34) Hamelin, A.; Martins, A. M. *J. Electroanal. Chem.* **1996**, *407*, 13.

JA106394K